UPPER BOUND ANALYSIS OF EXTRUSION OF I-SECTION BARS FROM SQUARE/RECTANGULAR BILLETS THROUGH SQUARE DIES

P. K. KAR and N. S. DAS

Department of Mechanical Engineering, Regional Engineering College, Rourkela - 769 008, India

Published in International Journal of Mechanical Sciences, 1997, Vol 39, Iss 8 P 925-934

Abstract—In the present study the SERR technique has been reformulated to deal with extrusion of sections with/without re-entrant corners. A comprehensive computational model has been developed for this reformulated technique. The model has been used to analyse extrusion of I-section bars and the computed results have been compared with experimental values available in literature.

Keywords: metal-forming, extrusion, three-dimensional, SERR technique.

NOMENCLATURE

a_i, b_i, c_i	coefficients in the equation to the plane containing the ith triangular face of a tetrahedron
A_i	area of the ith triangular face in the assembly of tetrahedrons
A_b	cross-sectional area of the billet
N	total number of faces in the assembly of tetrahedrons
P_{av}	average extrusion pressure
V_b	prescribed velocity of the billet
σ_0	yield stress in uniaxial tension
ϕ	function representing the equation of a plane
$\lvert\Delta v_i\rvert$	absolute velocity discontinuity at the ith face
∇	vector operator, $\hat{i}\frac{\partial}{\partial x}+\hat{j}\frac{\partial}{\partial x}+\hat{k}\frac{\partial}{\partial x}$

1. INTRODUCTION

Upper bound analysis of three-dimensional metal forming processes in general and extrusion in particular attracted great attention in the late 1960s and early 1970s. A number of techniques have since then been proposed to generate kinematically admissible velocity fields for such analyses. These include the Dual Stream Function method of Nagpal and Altan [1], and Nagpal [2], the Conformal Transformation technique and the Generalized Velocity Field technique of Yang *et al.* [3–6] and the method of proportional deformation developed by Gunasekara and Hoshino [7, 8]. However, all these techniques have been used to-date to analyse problems where any intermediate section in the deformation zone can be expressed as a continuous function of the space co-ordinates. When the extruded product involves singularities in the form of re-entrant corners (such as I- and T-sections), applying these methods may lead to considerable difficulties.

In a later paper, Gatto and Giarda [9] proposed a method for constructing kinematically admissible discontinuous velocity fields for upper bound analysis of three-dimensional plastic deformation problems. This method, known as the SERR (Spatial Elementary Rigid Regions) technique, is a generalization of the PERR (Planar Elementary Rigid Regions) method devised to analyse plane strain deformation problems [9]. The SERR technique envisages the deformation zone to consist of elementary rigid blocks separated by planes of velocity discontinuity. This process of discretisation into rigid blocks allows the spatial components of the internal velocity vector to be determined from the mass continuity condition applied at the bounding faces of the rigid blocks. Therefore the blocks must be necessarily tetrahedral in shape. This procedure was used by the above authors to find upper bound solutions for extrusion of polygonal bars from corresponding polygonal billets. However, their formulation appears to be unsuitable for analysing extrusion processes when the product and the billet have different sections, especially when the product section has re-entrant corners. The purpose of the present study is to reformulate the SERR technique so that it can be applied to analyse extrusion of bars of any cross section from billets of any other cross section

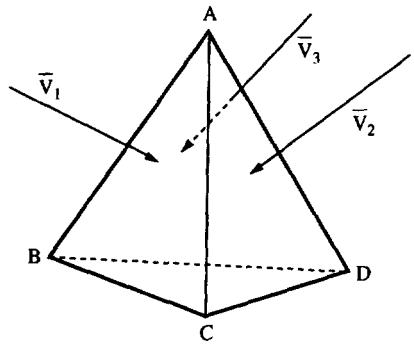

Fig. 1.

when the product and billet boundaries are defined by planar surfaces. The new formulation is then used to analyse the extrusion of I-section bars from square or rectangular billets. However, round billets have been excluded from this study because of the difficulty in having planar bounding faces for the SERR blocks in this case unless simplifying approximations are made.

2. THE VELOCITY FIELD IN AN SERR

We consider a tetrahedral block (Spatial Elementary Rigid Region) ABCD as shown in Fig. 1 with velocity vectors $\bar{V}_1$, $\bar{V}_2$, and $\bar{V}_3$ prescribed on the planar faces ABC, ACD, and ABD respectively. Let the velocity vector internal to this block be $\bar{V}$. According to Gatto and Giarda [9], $\bar{V}$ can be determined by a simple graphical construction. Alternatively, $\bar{V}$ can be determined by applying the mass continuity condition to the bounding faces of the tetrahedron and then simultaneously solving the resultant set of velocity equations outlined.

Let the equation of the plane containing the ith face of the tetrahedron ABCD be

$$\phi_i \equiv a_i x + b_i y + c_i z + 1 = 0 \tag{1}$$

Then the mass continuity condition can be applied to this face in the form

$$\bar{V}_i \cdot \hat{n}_i = \bar{V} \cdot \hat{n}_i, \quad i = 1, 2, 3 \tag{2}$$

where $\hat{n}_i$ is the unit normal vector associated with the ith face given by

$$\hat{n}_i = \frac{\nabla \phi_i}{|\nabla \phi_i|} \tag{3}$$

The coefficients a_i, b_i, and c_i in Eqn (1) for the plane containing the ith face can be obtained using the co-ordinates of the vertices of the tetrahedron. Then the three velocity equations generated by applying the continuity relation [Eqn (2)] give the three components of $\bar{V}$ on solution. This analytic procedure is well-suited for implementation on a digital computer.

3. THE DISCRETISATION PROCESS

The deformation zone in case of metal forming that occurs in a closed channel (like extrusion) may be subdivided into regions that are prismatic, pyramidal or tetrahedral in shape or a combination of these shapes. Since the elementary blocks are to be tetrahedral, the prismatic or pyramidal subzones are ultimately discretised into tetrahedrons. A pyramid can be discretised into two tetrahedrons by dividing the quadrilateral base into two triangles. Thus there are two ways of discretising the pyramid into tetrahedral blocks. The two tetrahedrons of a pyramid together have seven planar faces [represented by equations such as Eqn (1)] and hence seven velocity equations can be generated by applying the mass continuity condition to these faces. The number of unknown velocity components is also seven, six for the two internal velocity vectors associated with the two tetrahedrons and one for the exit velocity (whose direction is known from the physical description of the problem). In the same way, a prismatic subzone can be discretised into three tetrahedrons in six

different ways. The prismatic subzone has three internal velocity vectors and 10 independent faces that generate 10 velocity equations to uniquely establish the 10 velocity components (nine for the three internal velocity vectors and one at the exit) for this subzone.

4. DISCRETISATION OF THE DEFORMATION ZONE OF THE I-SECTION

The geometry for the extrusion of an I-section from a square or rectangular billet through a rough square die is shown in Fig. 2. The die faces being rough, dead metal zones are assumed to form on the die faces in the manner shown in the figure. From the consideration of symmetry only one-quarter of the deformation volume is taken as the domain of interest for the present analysis as shown in Fig. 3.

To visualise the way the deformation zone is discretised in the present analysis, we refer to the discontinuous velocity fields used for computing upper bound loads for the corresponding plane strain problem [10]. These are shown in Figs 4(a, b). The deformation zone shown in Fig. 4(a) consists of a single rigid triangle ABC obtained by joining the dead metal boundary AB with point C on the axis of symmetry. The deformation zone in Fig. 4(b) consists of two rigid triangles ABD and

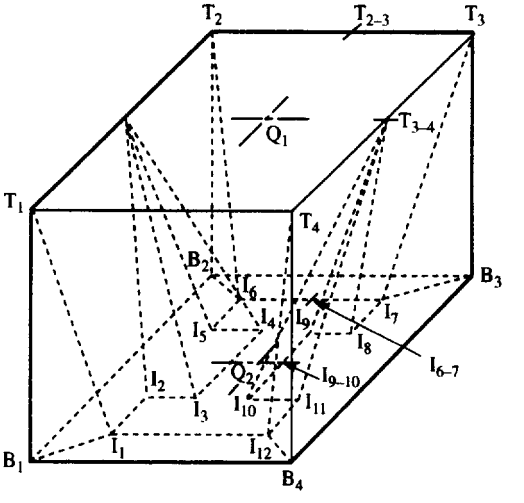

Fig. 2.

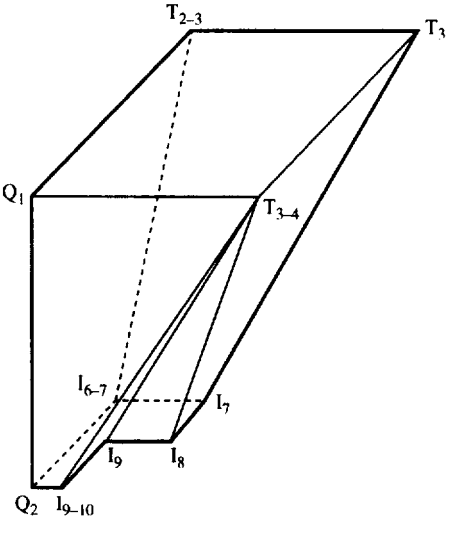

Fig. 3.

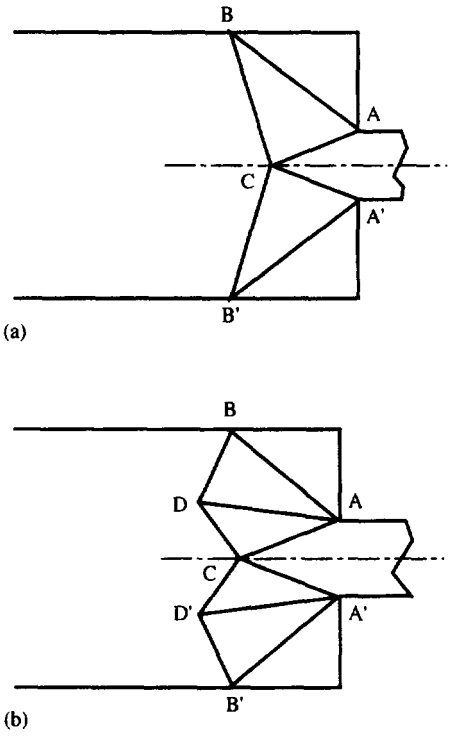

Fig. 4.

ADC where AB is the dead metal boundary, C is a point on the axis of symmetry and D is a point on the plane of extrusion as shown. The co-ordinates of the points B and C in Fig. 4(a) and points B,C, and D in Fig. 4(b) are the optimisation parameters with respect to which the extrusion pressure is minimised. In the present three-dimensional analysis, points like C and D are referred to as floating points, while co-ordinates of points such as B represent the height of the dead metal zone.

The above approach is extended to formulate kinematically admissible velocity fields for the present three-dimensional problem by suitably choosing floating points on the extrusion axis and elsewhere in the deformation cavity as demonstrated in Figs 5(a,b,c).

The velocity field shown in Fig. 5(a) is obtained when a single floating point on the extrusion axis is joined with dead metal boundaries as shown (Single Point Formulation). It is clear from this figure that the deformation zone in this case consists of two pyramidal subzones and two tetrahedral subzones. Since each pyramid can be discretised into two tetrahedrons, the entire deformation zone is discretised into six tetrahedral rigid blocks (or SERR) in four ways ($2 \times 2 \times 1 \times 1$). The best discretisation scheme is obviously the one that gives the lowest upper bound.

When two floating points (Double Point Formulation) are used as in Fig. 5(b), the deformation zone is subdivided into three pyramids and one tetrahedron. Thus there are seven tetrahedral rigid blocks which can be chosen in eight different ways ($2 \times 2 \times 2 \times 1$). As before the best discretisation scheme is the one giving the lowest upper bound.

When three floating points (Triple Point Formulation) are taken as shown in Fig. 5(c), the deformation zone gets subdivided into one prismatic and three pyramidal subzones. These subzones can be discretised into nine tetrahedral rigid blocks in 48 different ways ($6 \times 2 \times 2 \times 2$) and the best discretisation scheme is that which gives the lowest upper bound. Table 1 gives the summary of the discretisation details for the three formulations discussed above.

In the above model it has been assumed that the dead metal surface corresponding to the web of the I-section diverges from a single point, T_{3-4}. In order to make the model more general, the triple point formulation was modified by taking two extra points T_{x1} and T_{x2} on the line segment $T_{3-4}T_3$. It was assumed that points T_{x1}, T_{x2} and T_{3-4} corresponded to points I_8, I_9 and I_{9-10} respectively on the die orifice. As a result of this modification in the model, the shapes of the

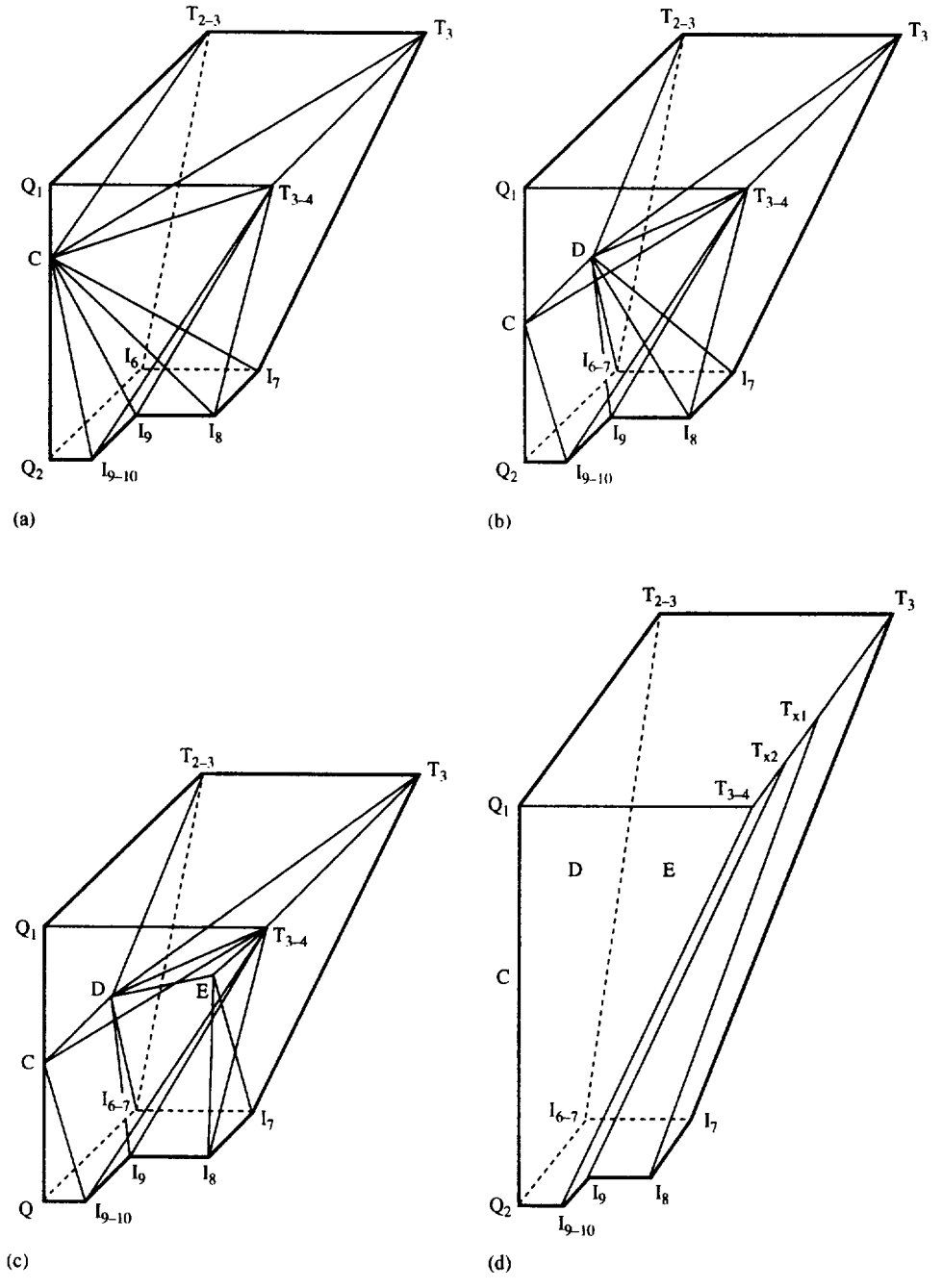

Fig. 5.

subzones of deformation changed and the number of SERR blocks increased as shown in Fig. 5(d) and summarised in Table 1. For the 11 tetrahedral blocks that resulted due to this modification, there were 34 independent bounding faces generating 34 velocity equations.

For easy visualisation of the metal flow and the relation existing among the various internal velocity vectors, the prismatic subzone $T_{2-3}T_{6-7}DT_3I_7E$ is isolated from Fig. 5(c) and redrawn in Fig. 6(a). The characteristics of the faces constituting this subzone are explained in the figure itself. The discretisation of this subzone into three tetrahedral blocks according to a typical scheme is shown in Fig. 6(b). In tetrahedron $T_{2-3}T_3I_{6-7}D$, face $T_{2-3}I_{6-7}D$ lies on a plane of symmetry. So the internal velocity vector for this SERR block is parallel to the plane $T_{2-3}T_3D$. Secondly, the face $T_{2-3}T_3I_{6-7}$ is a dead metal face admitting no mass flow in direction normal to itself. Hence the internal velocity vector is also parallel to this face. These conditions are enforced by taking the right

Table 1. Summary of discretisation schemes

Item	Formulation			
	Single point	Double point	Triple point	Modified triple point
Types of subzones	2 pyramids, 2 tetrahedron	3 pyramids, 1 tetrahedron	1 prism, 3 pyramids	3 prism, 1 pyramid
Total No. of rigid blocks	$2+2+1+1=6$	$2+2+2+1=7$	$3+2+2+2=9$	$3+2+3+3=11$
No. of discretisation schemes	$2\times2\times1\times1=4$	$2\times2\times2\times1=8$	$6\times2\times2\times2=48$	$6\times2\times6\times6=432$
No. of trianglular faces	19	22	28	34
No. of velocity components	$6\times3=18$ for 6 SERR and 1 at exit Total = 19	$7\times3=21$ for 7 SERR and 1 at exit Total = 22	$9\times3=27$ for 9 SERR and 1 at exit Total = 28	$11\times3=33$ for 11 SERR and 1 at exit Total = 34

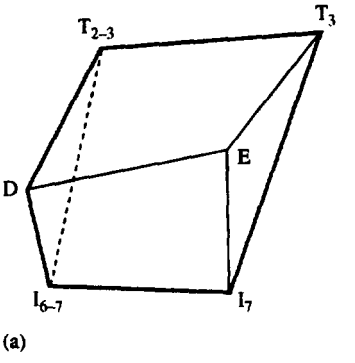

Fig. 6.

hand side equal to zero when Eqn (2) is applied to these faces. Thirdly, the face $T_{2-3}T_3D$ is one of the planes through which the billet enters the deformation zone. So the internal velocity vector is related to the billet velocity by applying Eqn (2) to this face. Finally, the plane $DI_{6-7}T_3$ is an internal plane separating the first and second tetrahedrons of the subzone under consideration. Thus the internal velocity vector of the first tetrahedron is related to that of the second by applying Eqn (2) to

the connecting face DT_3I_{6-7}. Similarly, the internal velocity vector for the second tetrahedron is related to that of the third by applying Eqn (2) to the connecting plane $I_{6-7}T_3E$. Continuing in this way, the internal velocity vector for the first tetrahedron of the second subzone (pyramid $T_3T_{3-4}I_8I_7E$) is related to that of the third tetrahedron of the first subzone by applying Eqn (2) to the connecting face T_3I_7E. In this manner all internal velocity vectors are inter-related through application of Eqn (2) to different faces of all the SERR blocks in the global system. The exit velocity is related to the internal velocity vector of a tetrahedron if an exit plane contains one of the faces of this tetrahedron.

5. COMPUTATION

A comprehensive computational model was developed to make an upper bound analysis of extrusion of I-sections using all the formulations discussed in the last section. The computation consisted of the following steps:

(1) determination of the equations of the planes containing the triangular faces of all the global level tetrahedrons using the co-ordinates of the respective vertices. [This amounted to determining the coefficients a_i, b_i and c_i in Eqn (1) for all the faces];
(2) determination of the velocity equations by applying the mass continuity condition to all the faces;
(3) simultaneously solving the velocity equations to determine all the internal velocity components with the billet velocity as an input data. (The solution also determined the exit velocity. This served as a check on computation since exit velocity can be independently calculated using the billet velocity and the area reduction);
(4) calculation of the non-dimensional average extrusion pressure from the relation

$$\frac{P_{av}}{\sigma_0} = \frac{1}{\sqrt{3}} \times \frac{1}{A_b \times V_b} \sum_{i=1}^{N} A_i \times |\Delta V_i| \tag{4}$$

where: N = no of global level triangular faces,
$|\Delta V_i|$ = velocity discontinuity at the ith face
A_i = area of the ith face,
σ_0 = yield stress in uniaxial tension,
A_b = area of billet cross section, and
V_b = billet velocity;

(5) optimisation of the average extrusion pressure using a multivariate unconstrained optimisation routine.

6. THE OPTIMISATION PARAMETERS

For the single point formulation, the floating point lies on the extrusion axis (taken as the z-axis). Thus it has a single undetermined co-ordinate. Further, the height of the dead metal zone (which is the z-coordinate of the points of intersection of the dead metal faces and the container wall) is another undetermined parameter. These two undetermined quantities serve as the optimisation parameters to minimise the extrusion pressure for this formulation.

In case of the double point formulation, there are two floating points, one on the extrusion axis (z-coordinate undetermined) and the other on the plane of symmetry (y- and z-coordinates undetermined). These three undetermined coordinates along with the height of the dead metal zone serve as the four optimization parameters for this formulation.

In case of the triple point formulation, the first two floating points (located as in double point formulation) together have three undetermined coordinates while the third floating point arbitrarily located in the deformation cavity has three undetermined coordinates. These six coordinates along with the height of the dead metal zone serve as the seven optimisation parameters for this formulation.

In case of the modified triple point formulation of Fig. 5(d), the number of optimisation parameters is nine since the points T_{x1} and T_{x2} have only one undetermined coordinate each (the y-coordinate) and these two are included in the list of parameters of the triple point formulation.

7. RESULTS AND DISCUSSION

Computations were carried out for all the four global discretisation schemes of the single point formulation and the scheme giving the least upper bound was identified. The discretised deformation zone corresponding to the least upper bound is named here as the optimum configuration. The optimum configurations in case of double point and triple point formulations were similarly determined. Table 2 gives a comparison of the computed results of the three formulations for their respective optimum configurations. It is obvious from this table that the triple point formulation gives the best results. Therefore this formulation only is used for further computation.

Assuming the product aspect ratio (overall length of the I-section divided by its overall breadth) to be one, computations were made to study the effect of billet aspect ratio on the average extrusion pressure. The results are presented in Table 3 for four billet aspect ratios. It is seen that the extrusion pressure slightly decreases with increase in billet aspect ratio. This is probably due to the fact that at higher billet aspect ratios, the dead metal zones are thinner on the sides having the re-entrant corners which in turn reduces the redundant work.

Provision was made in the present model to study the effect of the inherent asymmetry of the I-section by taking unequal heights for the corner points like T_{2-3}, T_3, T_{3-4} [Fig. 5(c)]. These heights were included in the list of optimisation parameters. However, it was seen that introduction of unequal corner heights had marginal effect on the non-dimensional average extrusion pressure as shown in Table 4.

When the modified triple point formulation of Fig. 5(d) was implemented, it was observed that the distances $T_{3-4}T_{x1}$ and $T_{3-4}T_{x2}$ (which happen to be the y-coordinates of points T_{x1} and T_{x2} respectively) became negligibly small corresponding to minimum extrusion pressure. These distances, for a typical global scheme of discretisation, became of the order of 10^{-3} when the billet dimension was of the order of 20. Also, there was no significant reduction in the value of the non-dimensional average extrusion pressure. For some optimisation schemes, these distances became so small that the points T_{x1} and T_{x2} converged to T_{3-4} and triangular faces like $ET_{x2}T_{x1}$ and $ET_{3-4}T_{x2}$ became straight lines giving rise to breakdown of the procedure since spatial tetrahedrons degenerated to planar triangles. So this modification was not pursued any further.

Table 2. Comparison of results for the three formulations

Area reduction (%)	Non-dimensional average extrusion pressure, P_{av}/σ_0		
	Single point	Double point	Triple point
70	6.980	3.648	3.289
75	7.680	4.044	3.681
80	8.779	4.569	4.215
85	10.414	5.304	4.968
90	13.162	6.440	6.137

Table 3. Effect of billet aspect ratio on non-dimensional average extrusion pressure, P_{av}/σ_0

Area reduction (%)	Non-dimensional average extrusion pressure, P_{av}/σ_0			
	Billet aspect ratio = 1.0	Billet aspect ratio = 1.1	Billet aspect ratio = 1.2	Billet aspect ratio = 1.25
60	2.832	2.689	2.638	2.784
65	3.008	2.883	2.814	2.802
70	3.289	3.174	3.108	3.094
75	3.681	3.578	3.521	3.508
80	4.215	4.128	4.081	4.070
85	4.968	4.896	4.858	4.849
90	6.137	6.075	6.004	6.088

Table 4. Effect of unequal corner heights on non-dimensional average extrusion pressure, P_{av}/σ_0

Area reduction (%)	P_{av}/σ_0	
	Equal corner height	Unequal corner height
70	3.289	3.261
75	3.681	3.666
80	4.215	4.205
85	4.968	4.957
90	6.137	6.121

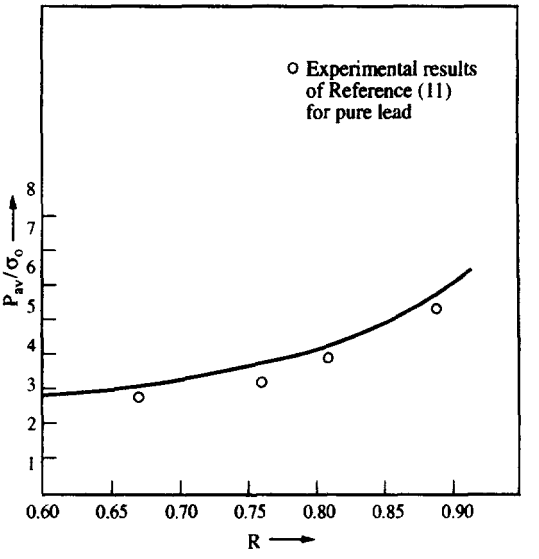

Fig. 7.

Finally, the average extrusion pressures computed in this study are compared with the experimental results of Chitkara and Adeyemi [11] in Fig. 7. It is seen that there is good agreement between the two. The slightly higher values obtained by this study may be due to the fact that the computed results give upper bounds rather than the exact.

In conclusion it can be stated that:

(1) among the three SERR formulations carried out in this study, the triple point formulation gives the lowest upper bound to the extrusion pressure for extruding I-section bars;
(2) the least upper bounds computed agree well with experimental results available in literature;
(3) the extrusion pressure reduces marginally if billet aspect ratio is slightly higher than the product aspect ratio.

REFERENCES

1. Nagpal, V. and Altan, T., *Proceedings of the Third North American Metalworking Research Conference*, Carnegie-Melon University, Pittsburgh, PA, May, 1975.
2. Nagpal, V., *Trans. ASME, SER B*, 1977, **99**.
3. Yang, D. Y. and Lee, C. H., *Int. J. Mech. Sci.*, 1978, **20**, 541.
4. Yang, D. Y., Kim, M. U. and Lee, C. H., *Int. J. Mech. Sci.*, 1978, **20**, 695.
5. Han, C. H., Yang, D. Y. and Kiuchi, M., *Int. J. Mech. Sci.*, 1986, **28**, 201.
6. Yang, D. Y., Han, C. H. and Kim, M. U., *Int. J. Mech. Sci.*, 1986, **28**, 517.

7. Gunasekara, J. S. and Hoshino, S., *Trans. ASME, SER B*, 1982, **104**, 38.
8. Gunasekara, J. S. and Hoshino, S., *Trans. ASME, SER B*, 1985, **107**, 229.
9. Gatto, F. and Giarda, A., *Int. J. Mech. Sci.*, 1981, **23**, 3.
10. Johnson, W. and Kudo, H., *The Mechanics of Metal Extrusion*. Manchester Univ. Press, Manchester, 1962.
11. Chitkara, N. R. and Adeyemi, M. B., *Proceedings, 8th IMTDR Conference*, London, 1977.